Supporting Information for
Ion Switchable Quantum Dot Förster Resonance Energy Transfer Rates In Ratiometric Potassium Sensors

Timothy T. Ruckh[1], Christopher G. Skipwith[1], Wendi Chang[2], Alexander W. Senko[3], Vladimir Bulovic[2], Polina O. Anikeeva[3], Heather A. Clark[1*]

[1] Department of Pharmaceutical Sciences, Northeastern University, 360 Huntington Ave, Boston, MA 02115

[2] Department of Electrical Engineering, Massachusetts Institute of Technology, 77 Massachusetts Avenue, Cambridge, MA 02139

[3] Department of Materials Science and Engineering, Massachusetts Institute of Technology, 77 Massachusetts Avenue, Cambridge, MA 02139

[*] H.clark@neu.edu

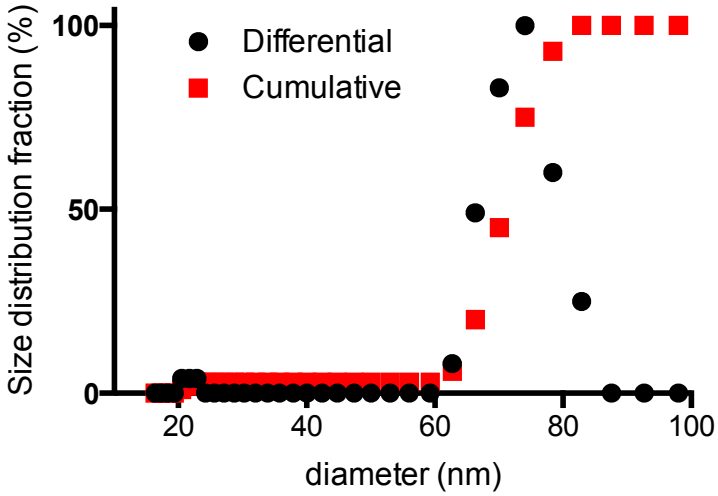

Figure S1 – Intensity-weighted nanoparticle diameter distribution measured by DLS.

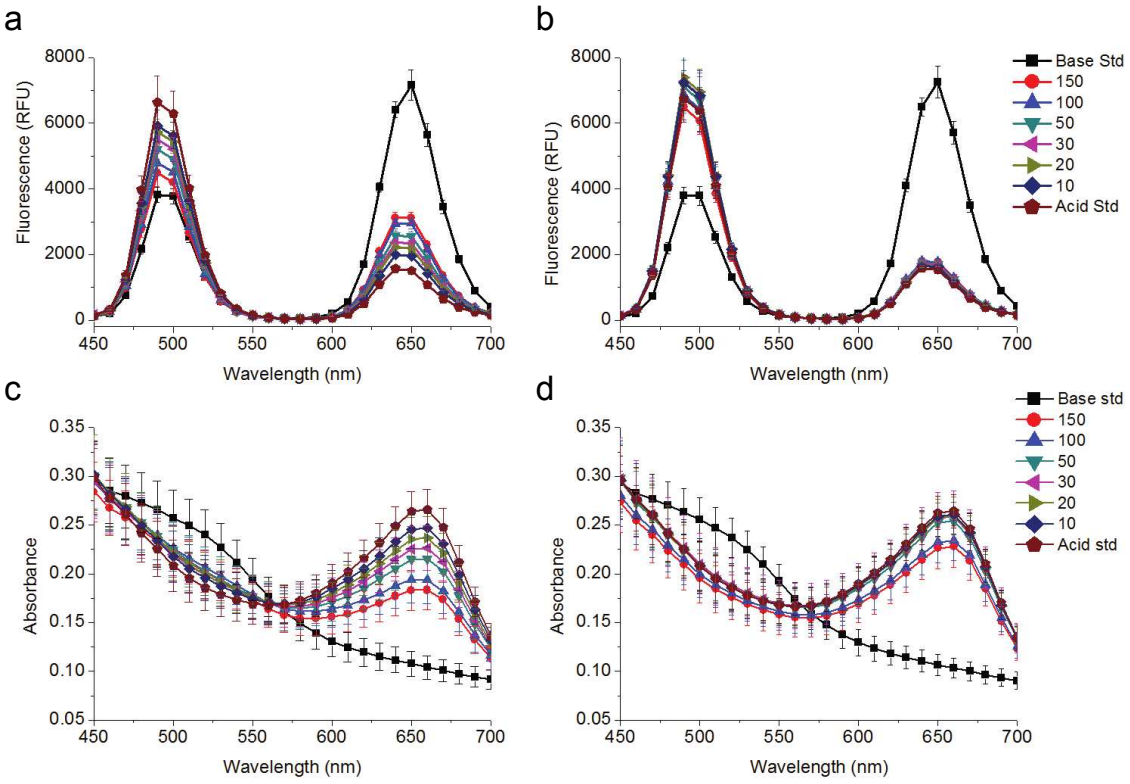

Figure S2 – Fluorescence spectra in response to potassium (a) and sodium (b) and the corresponding absorbance spectra in response to potassium (c) and sodium (d). Error bars in (d) indicate one standard deviation

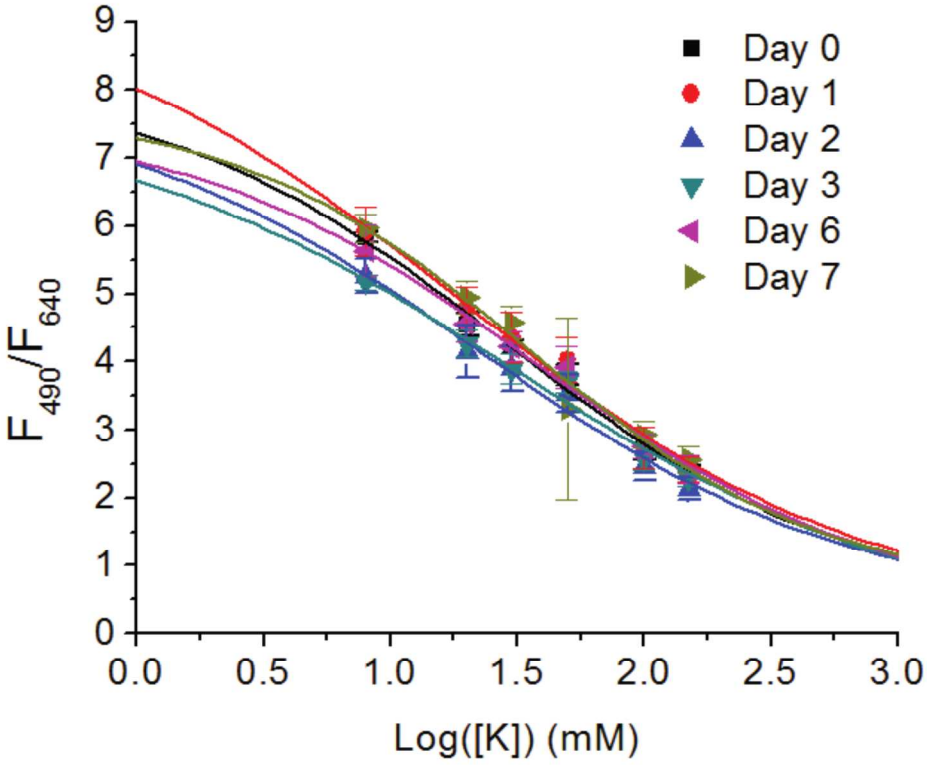

Figure S3 – Nanosensor shelf stability showing similar calibration responses from day 0 through day 7. Storage conditions were in room temperature and shielded from light. Error bars indicate one standard deviation

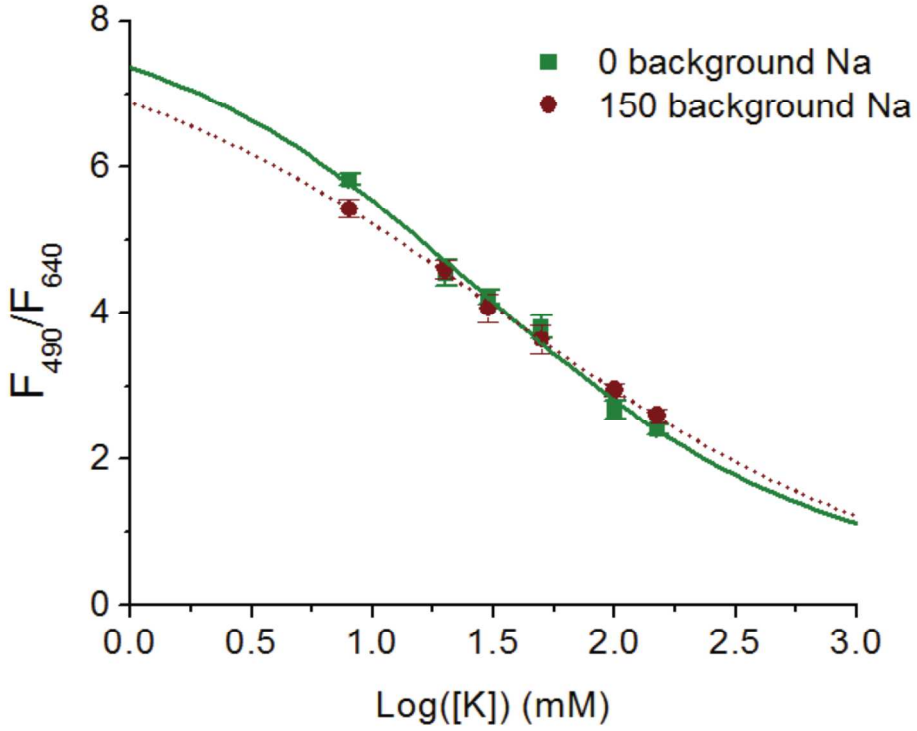

Figure S4 – Calibrations of nanosensors in 0 or 150 mM background Na. Error bars indicate one standard deviation

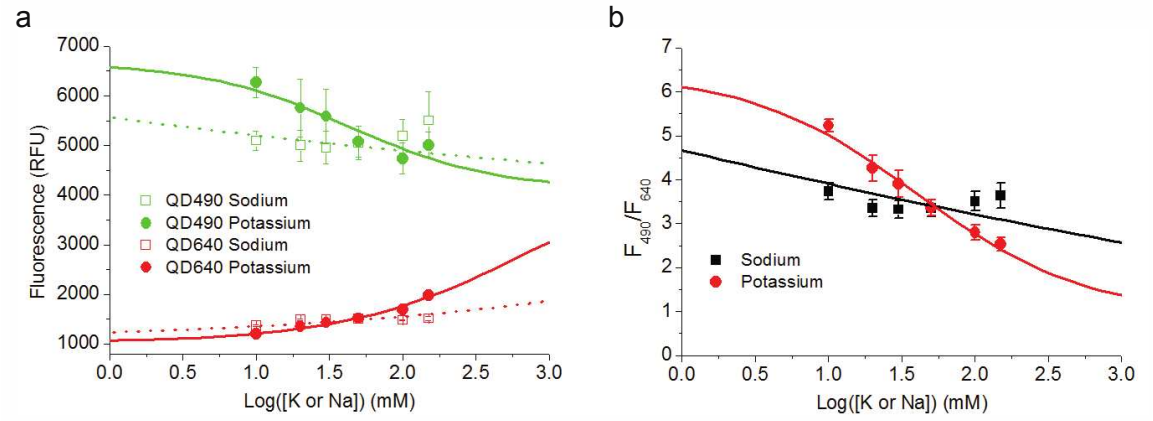

Figure S5 – Calibrations of nanosensors in 50 mM background ionic strength for responses to sodium or potassium. Individual channels (a) and the ratiometric measure (b) all show selective responses to potassium and no specific response to sodium. Error bars indicate one standard deviation

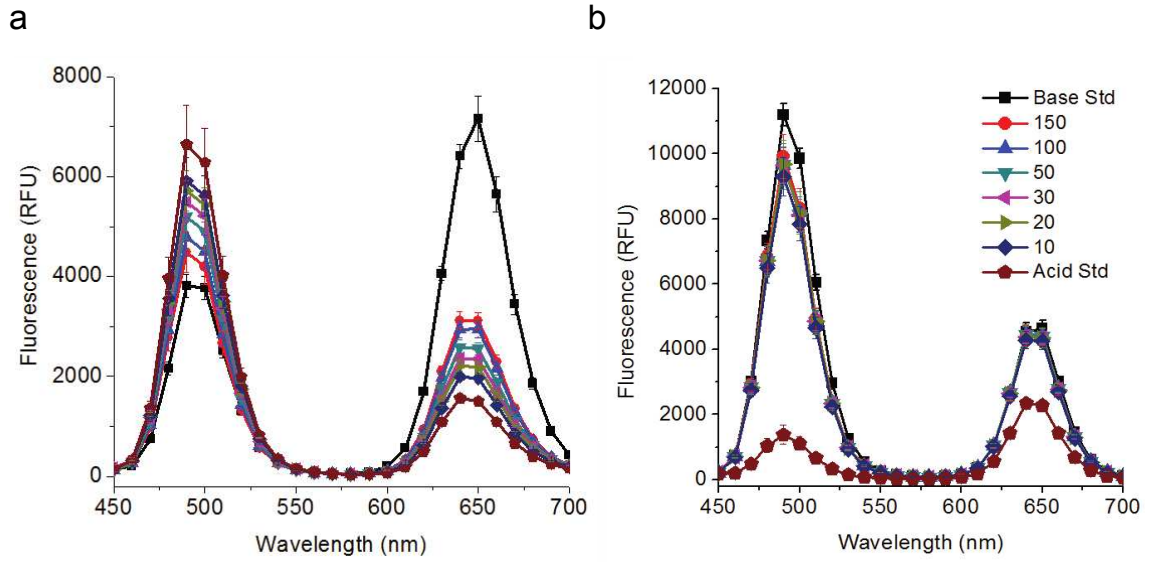

Figure S6 – Fluorescence spectra of potassium nanosensors made with (a) and without (b) chromoionophore showing that the quantum dots do not respond to potassium and the chromoionophore mediates the dynamic fluorescence response to potassium. Error bars indicate one standard deviation

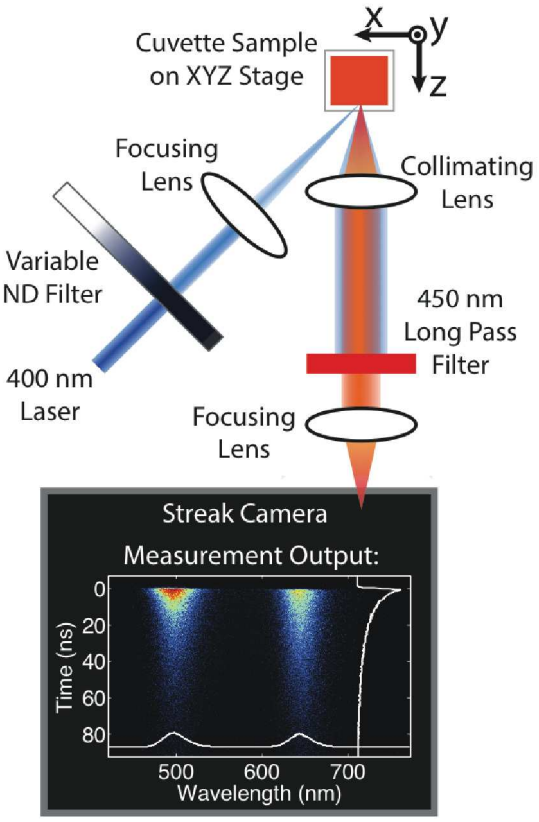

Figure S7 – Optical system for recording time-resolved spectra recorded from 440 nm to 780 nm over a 100 ns interval.

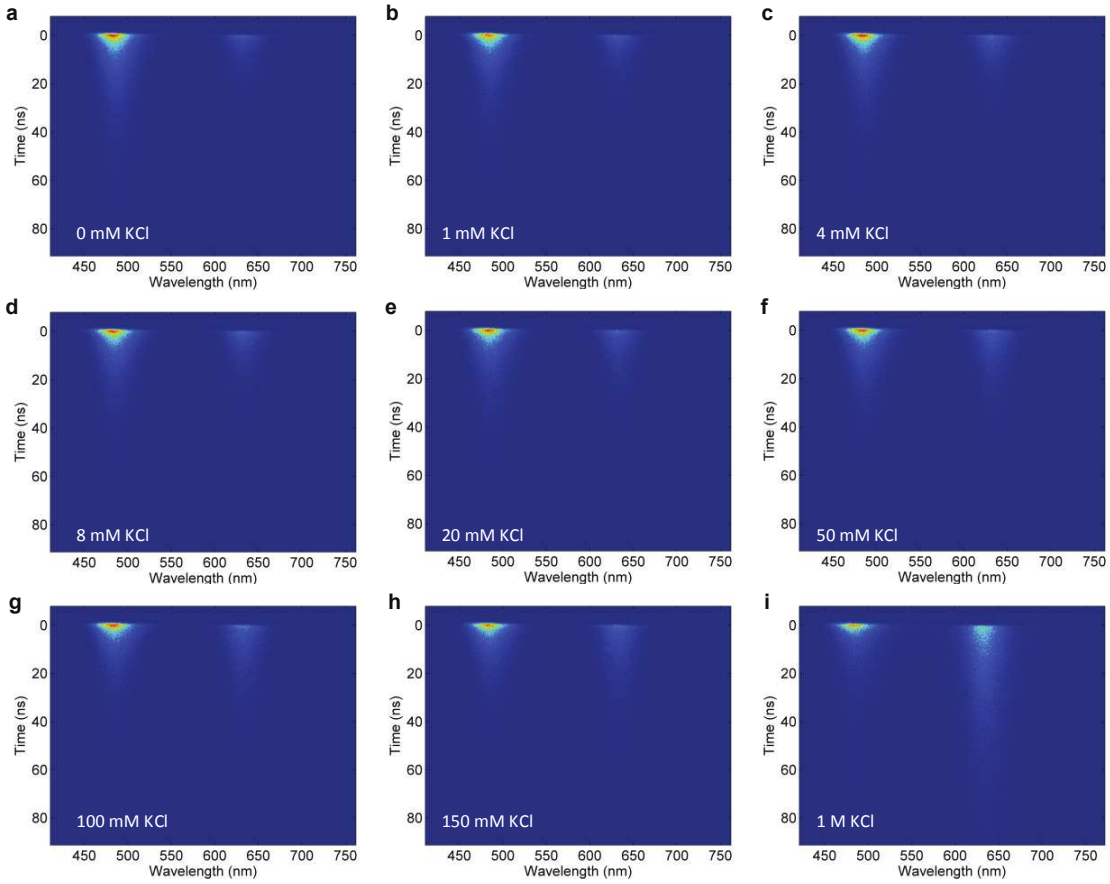

Figure S8 – Streak camera images from nanosensors in KCl solutions. Solution concentrations, in mM, of 0 (a), 1 (b), 4 (c), 8 (d), 20 (e), 50 (f), 100 (g), 150 (h), and 1000 (i) KCl.

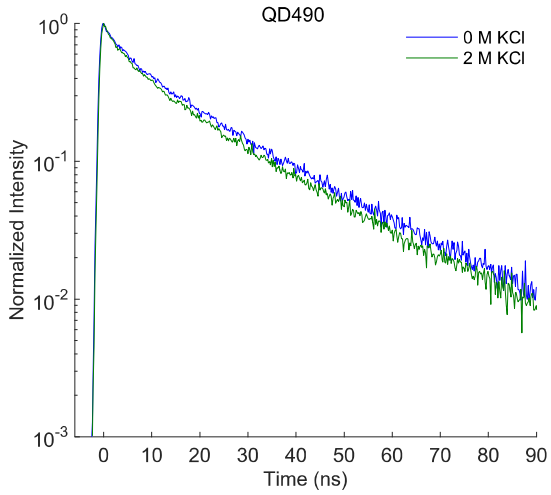
QD490
0 M KCl
2 M KCl
Normalized Intensity
Time (ns)

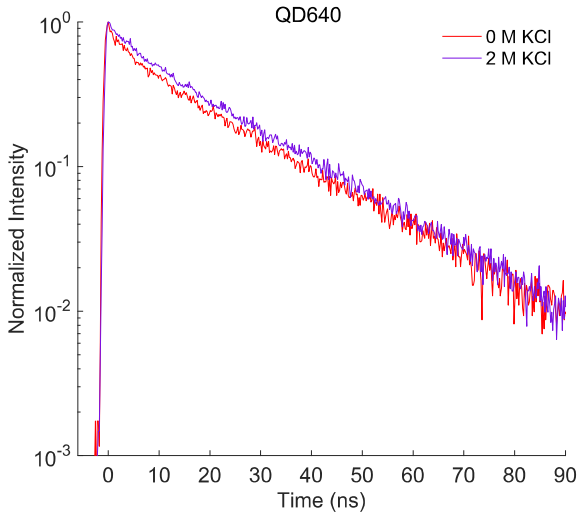
QD640
0 M KCl
2 M KCl
Normalized Intensity
Time (ns)

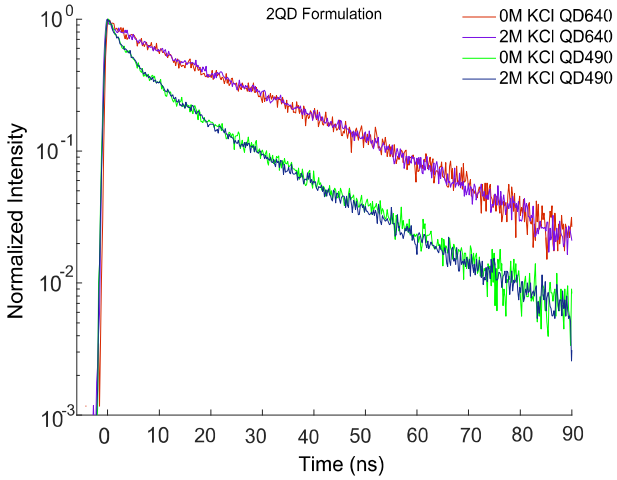
2QD Formulation
0M KCl QD640
2M KCl QD640
0M KCl QD490
2M KCl QD490
Normalized Intensity
Time (ns)

Figure S9 - Time-resolved fluorescence for nanosensors with QD490 (a), QD640 (b), and both QDs (c). None of these contained chromoionophore, and none exhibited any potassium dependent change in lifetime.

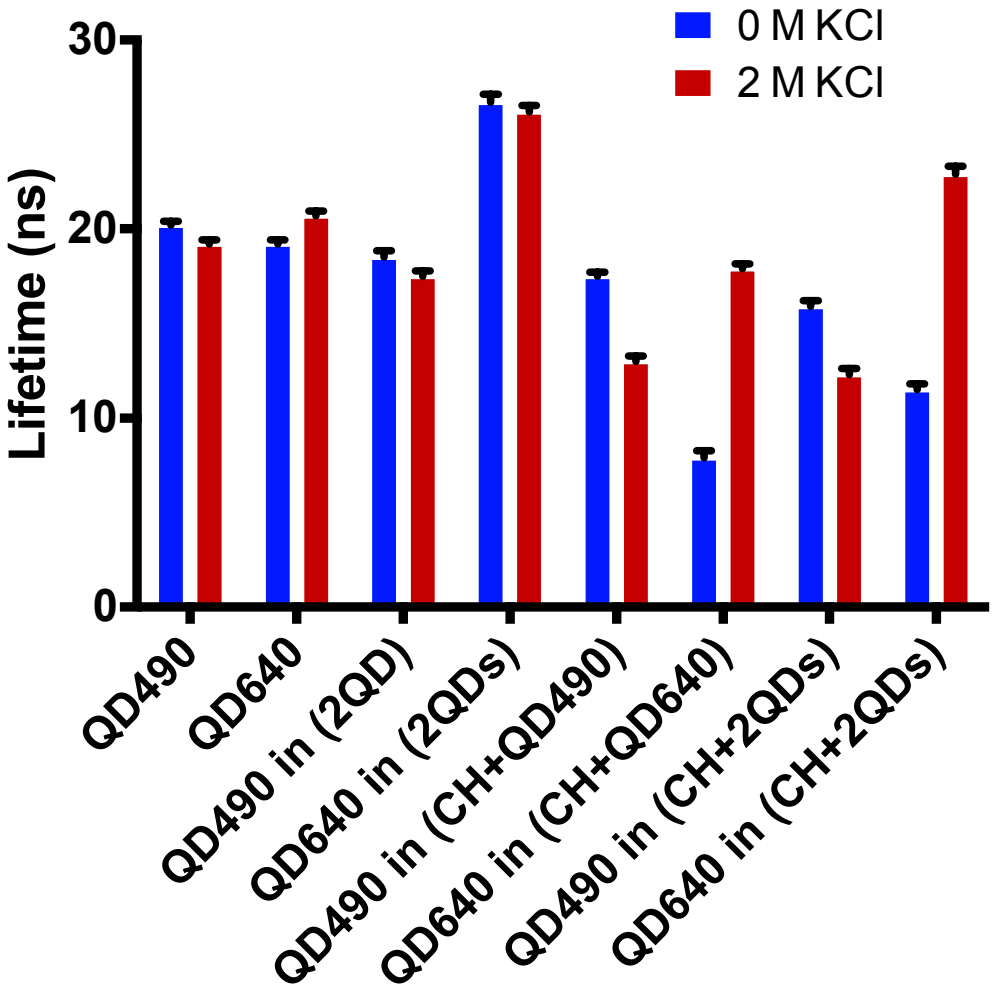

Figure S10 – Fluorescence lifetimes determined from fitting time-domain fluorescence images. X-axis indicates the component with the deconstructed nanosensor composition in parenthesis.

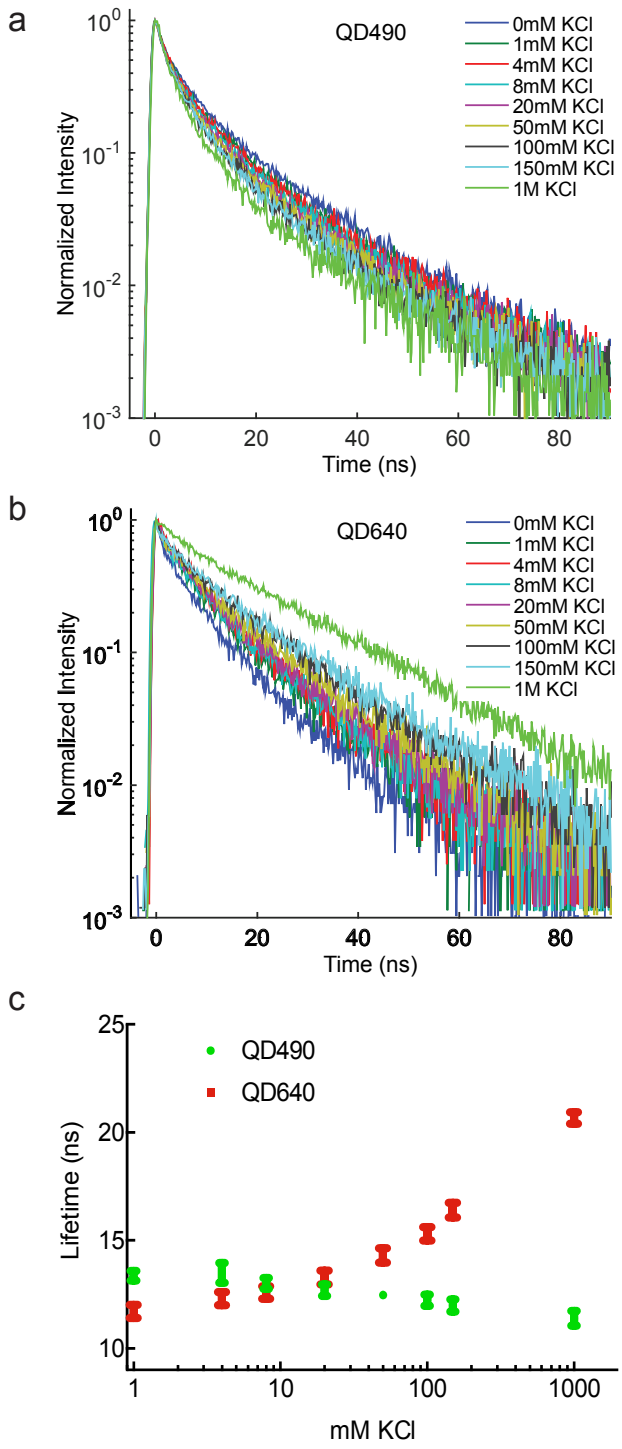

Figure S11 – Time-domain fluorescence lifetimes for QD490 (a) and QD640 (b) showing potassium-dependent fluorescence. Lifetimes are plotted against potassium concentration (c). Error bars indicate one standard deviation

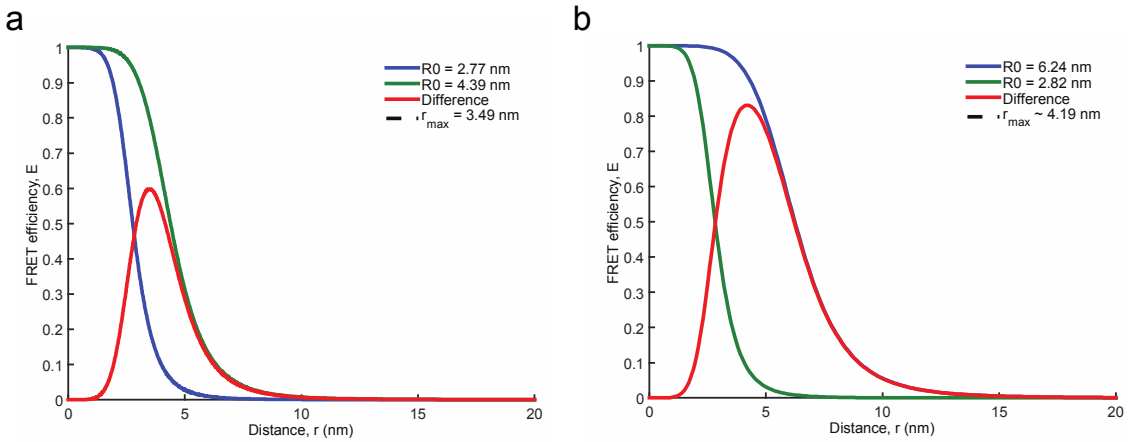

Figure S12 – FRET overlap integrals calculated from chromoionophore absorbance spectra and quantum dot emission spectra for QD490-CH (a) and QD640-CH (b). The difference in overlap integrals for the protonated CH case (blue lines) and deprotonated case (green lines) is also plotted to show the QD-CH spacing that will lead to maximal contrast between the two cases

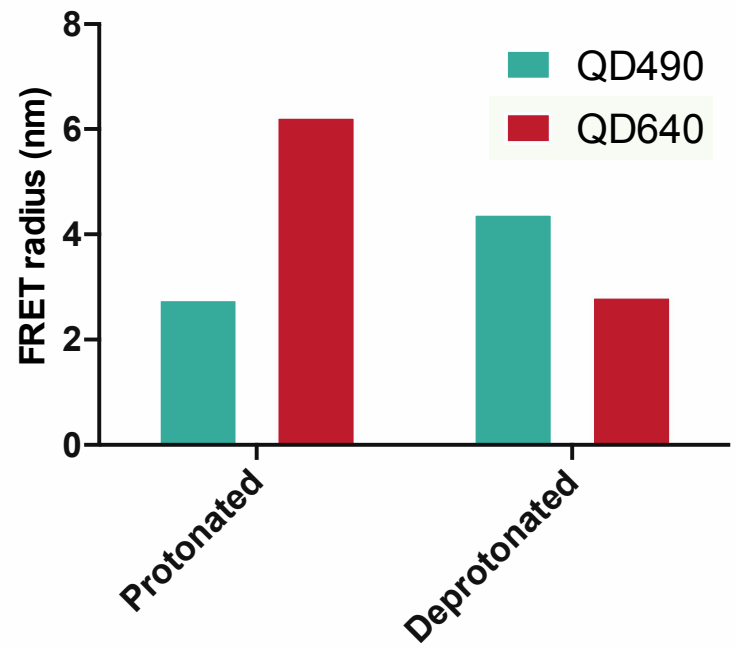

Figure S13 – FRET overlap integrals in the protonated and deprotonated chromoionophore cases predict the FRET radii from either QD to the chromoionophore in both conditions

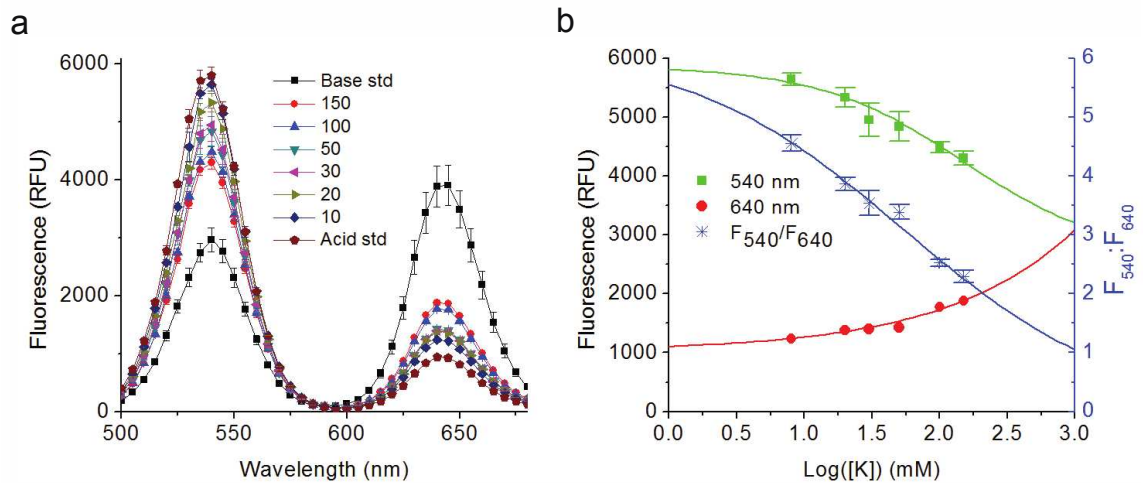

Figure S14 – Nanosensors made with QD540 and QD640. The fluorescence spectrum (a) and the resulting fitted calibration curves for both QDs and the ratiometric measure F_{540}:F_{640} (b). Error bars indicate one standard deviation

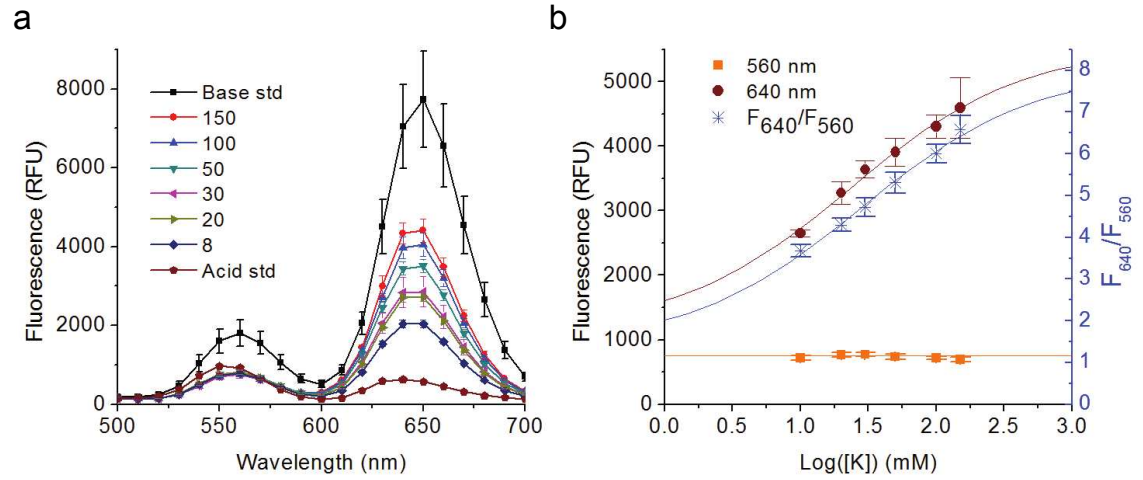

Figure S15 – Nanosensors with QD560 and QD640. The fluorescence spectrum (a) and the resulting fitted calibration curves for both QDs and the ratiometric measure F_{540}:F_{640} (b). The fabrication method was described in the methods, and the formulation consisted of 5 mg potassium ionophore II, 6 mg NaBARF, 500 μg Chromoionophore II, 200 μL nitrophenyl octyl ether. Each batch contained 60 μg QD560 and 189 μg QD640. Error bars indicate one standard deviation

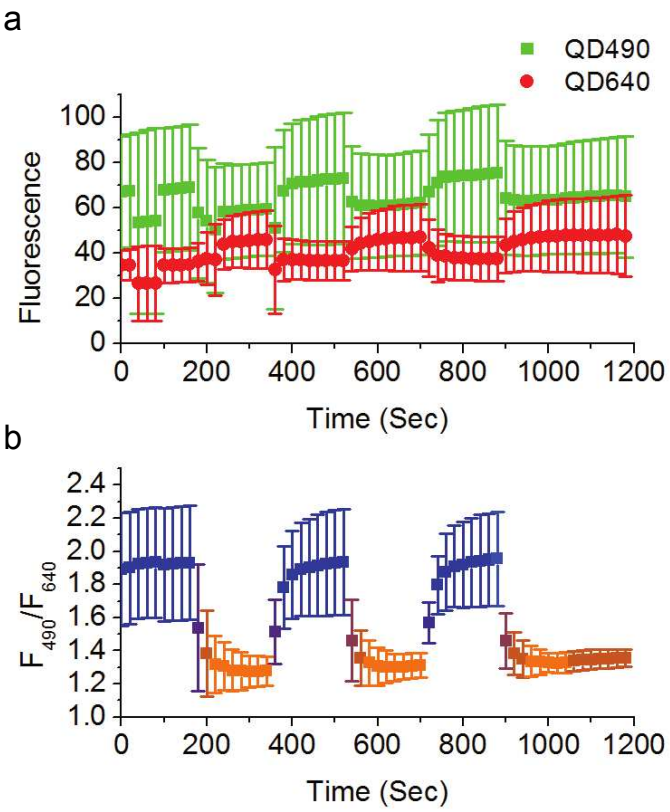

Figure S16 – Nanosensors are fully reversible for individual channels (a) and ratiometric signal (b) through over 20 minutes of imaging when exchanging solutions of 100 mM KCl (b, blue) or 10 mM KCl (b, orange) in a perfusion chamber. Error bars indicate one standard deviation

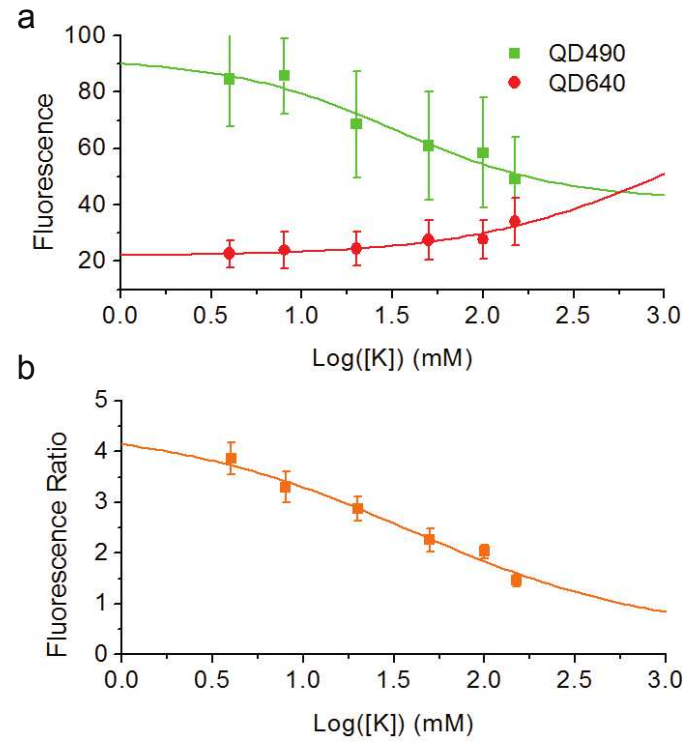

Figure S17 – Calibration curves fitted to data acquired by imaging nanosensors immobilized in dialysis tubing on a confocal microscope (Ex: 405 nm). Fluorescence from both QDs (a) and the intensity ratio (b) in response to potassium concentration. Error bars indicate one standard deviation

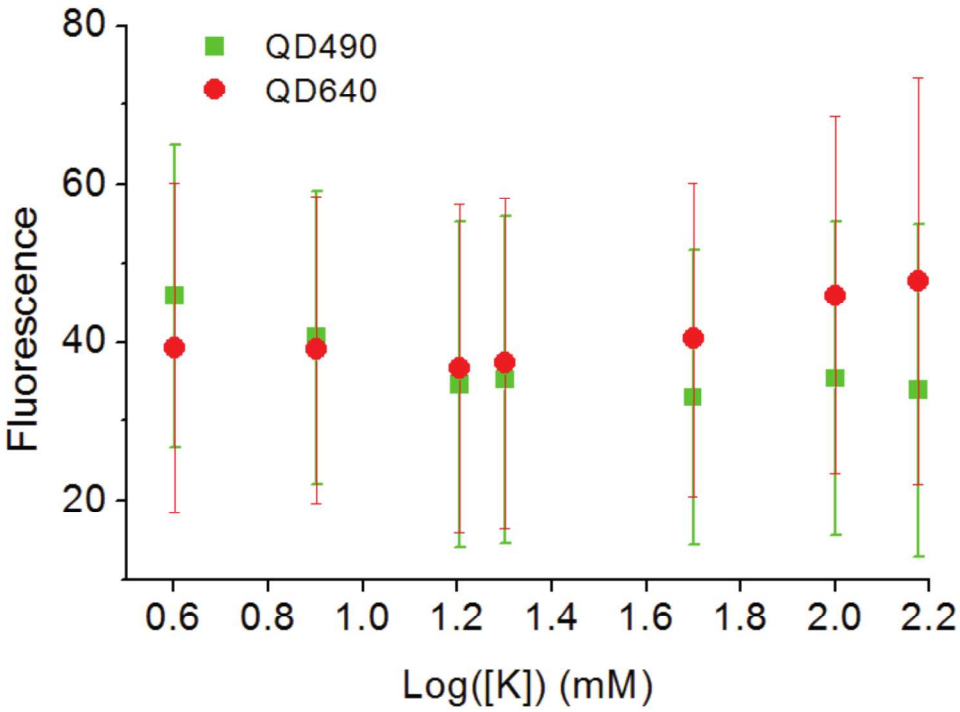

Figure S18 – *In situ* calibration measurements for individual QD channels recorded by perfusing potassium solutions into an imaging chamber. Error bars indicate one standard deviation

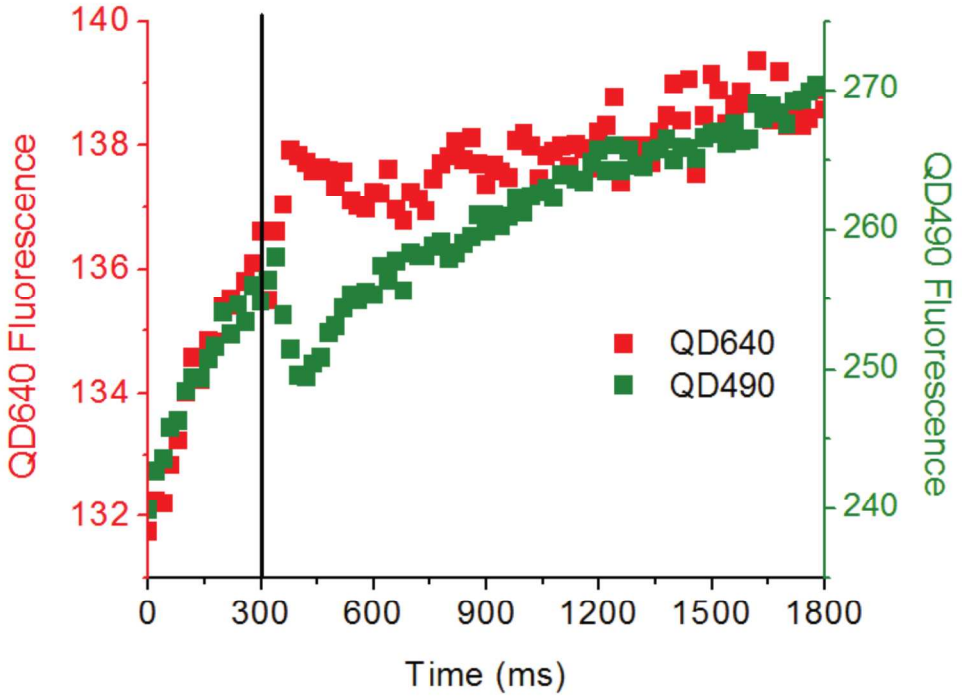

Figure S19 – Individual QD responses to a brief puff of 150 mM KCl. Each channel was imaged separately and the KCl delivery timing was matched (black vertical line) between trials